World Academy of Science, Engineering and Technology
International Journal of Electrical and Computer Engineering
Vol:9, No:6, 2015

Power Control of DFIG in WECS Using Backstipping and Sliding Mode Controller

A. Boualouch, A. Essadki, T. Nasser, A. Boukhriss, A. Frigui

***Abstract*—**This paper presents a power control for a Doubly Fed Induction Generator (DFIG) using in Wind Energy Conversion System (WECS) connected to the grid. The proposed control strategy employs two nonlinear controllers, Backstipping (BSC) and sliding-mode controller (SMC) scheme to directly calculate the required rotor control voltage so as to eliminate the instantaneous errors of active and reactive powers. In this paper the advantages of BSC and SMC are presented, the performance and robustness of this two controller's strategy are compared between them. First, we present a model of wind turbine and DFIG machine, then a synthesis of the controllers and their application in the DFIG power control. Simulation results on a 1.5MW grid-connected DFIG system are provided by MATLAB/Simulink.

***Keywords*—**Backstipping, DFIG, power control, sliding-mode, WESC.

NOMENCLATURE

ρ	Air Density (kg/m^3)
Ω_t	Tip Speed Ratio
λ	Turbine Radius
R	Rotor radius (m)
v	Wind speed (m/sec)
C_p	Power Coefficient
β	Pitch angle
T_{em}	Electromagnetic torque (Nm)
V_{ds}, V_{qs}	Direct and Quadratic Stator Voltages
V_{dr}, V_{qr}	Direct and Quadratic Stator Voltages
I_{ds}, I_{qs}	Direct and Quadratic Stator currents
I_{dr}, I_{qr}	Direct and Quadratic Stator currents
Φ_{ds} , Φ_{qs}	Direct, Quadratic Stator Flux (Wb)
Φ_{dr} , Φ_{qr}	Direct, Quadratic Rotor Flux (Wb)
P_s, Q_s	Active and reactive stator Power
P_{ref}, Q_{ref}	Reference active and reactive stator Power
R_r, R_s	Rotor and stator Resistance (Ω)
L_s, L_r, L_m	Stator, Rotor and mutual Inductance (H)
p	Pole pair number
θ_r	Rotor position
ω_s, ω_r	Synchronous and Angular speed
g	Slip

I. INTRODUCTION

THE wind energy conversion system WECS produce electricity from wind, it has several advantages, first it is an inexhaustible source, and then it does not pollute the environment, but in the other side, its cost remains high and its energy efficiency is still low compared to conventional sources [1], [2].

A. Boualouch, A. Essadki, T. Nasser, A. Boukhriss, and A. Frigui is with LGE Lab, Enset, University of Mohammed V, Rabat, Morocco (e-mail: abdellah.boualouch @um5s.net.ma, a.essadki @um5s.net.ma, t.nasser @um5s.net.ma, ali_boukhriss @live.fr, frigui.abdellatif @gmail.com).

The Doubly Fed Induction Generator (DFIG) is the most used in high power wind production. The stator of DFIG is directly related to grid side, the rotor is connected to the grid by two converters AC/DC/AC. The advantage of this type of machine is its ability to operate over a large range of wind speeds with a lower rotor converter [3]-[5].

A vector control scheme is applied to the DFIG, which makes the DFIG similar to DC machine; it allows a decoupling of the active and reactive power in the DFIG. In the proposed controller, the machine parameters must be determined exactly, because it is used to calculate the controller parameters. The controller's robustness is affected following changes in these parameters [4].

These last years, several researches are about the nonlinear controllers such us Backstipping (BSC) and sliding mode control (SMC) which have enjoyed great success in recent years for their simplicity of implementation and robustness against disturbances which may affect process[6]-[8].

In this article and after modeling the wind turbine and DFIG, we have established a vector control to control the active and reactive power control using a SMC and BSC. The aim of this work is to present the performance and robustness of these controllers.

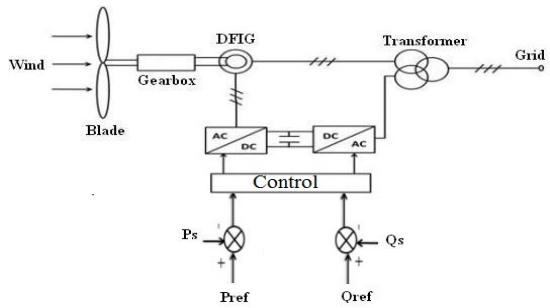

Fig. 1 Wind energy conversion system based on DFIG connected to the grid

II. TURBINE MODEL

The mechanical power transferred from the wind to the aerodynamic rotor is [9]:

$$P_{mt} = \frac{1}{2}\rho R^2 V^3 C_p(\lambda, \beta) \quad (1)$$

The input torque in the transmission mechanical system is then [10]:

$$T_t = \frac{\frac{1}{2}\rho R^2 V^3 C_p(\lambda,\beta)}{\Omega_t} \quad (2)$$

The power coefficient C_p of the wind turbine given by [11]:

$$C_p(\lambda,\beta) = 0.51\left(\frac{116}{\lambda i} - 0.4\beta - 5\right)e^{\frac{-21}{\lambda_i}} + 0.0068\lambda \quad (3)$$

$$\frac{1}{\lambda_1} = \frac{1}{\lambda + 0.08\beta} - \frac{0.035}{\beta^3 + 1} \quad (4)$$

Fig. 2 shows the power coefficient for different values of β.

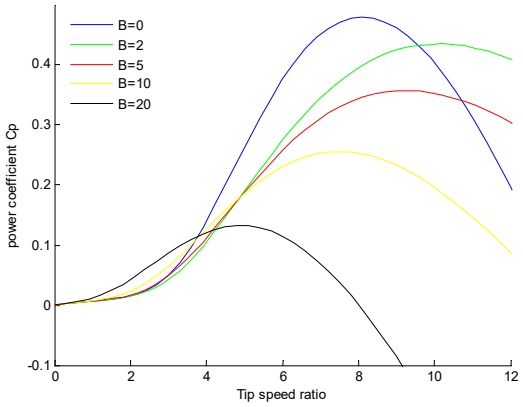

Fig. 2 Turbine Power coefficient

III. DFIG Model

The mathematical models of three phases DFIG in the Park frame are written as [7]-[10]:

$$\begin{cases} V_{ds} = R_s I_{ds} + \frac{d\Phi_{ds}}{dt} - \omega_s \Phi_{qs} \\ V_{qs} = R_s I_{qs} + \frac{d\Phi_{qs}}{dt} + \omega_s \Phi_{ds} \\ V_{dr} = R_r I_{dr} + \frac{d\Phi_{dr}}{dt} - \omega_r \Phi_{qr} \\ V_{qr} = R_r I_{qr} + \frac{d\Phi_{qr}}{dt} + \omega_r \Phi_{dr} \end{cases} \quad (5)$$

$$\begin{cases} \Phi_{ds} = L_s I_{ds} + L_m I_{dr} \\ \Phi_{qs} = L_s I_{qs} + L_m I_{qr} \\ \Phi_{dr} = L_r I_{dr} + L_m I_{ds} \\ \Phi_{qr} = L_r I_{qr} + L_m I_{qs} \end{cases} \quad (6)$$

The electromagnetic torques is expressed as [7], [9], [13]:

$$T_e = -\frac{3}{2} p \frac{L_m}{L_s}(\Phi_{ds} I_{dr} - \Phi_{qs} I_{ds}) \quad (7)$$

IV. Power Control Strategy

To simplify the study of the power control strategy, we use a vector control of DFIG based on stator field oriented (SFO), by setting the stator field aligned with d-axis [7], [10], [13]. We have:

$$\Phi_{sq}=0 \quad \text{and } \Phi_{sd}=\Phi_s \quad (8)$$

in this case the torque becomes:

$$T_e = -\frac{3}{2} p \frac{L_m}{L_s}(\Phi_{ds} I_{dr}) \quad (9)$$

This electro-mechanic torque and the reactive power depend only on the q-axis rotor current; the machines used in wind conversion are generally high power so we can neglect the stator resistance R_s [14]. We can write:

$$\begin{cases} \Phi_{ds} = \Phi_s = L_s I_{ds} + L_m I_{dr} \\ \Phi_{qs} = 0 = L_s I_{qs} + L_m I_{qr} \end{cases} \quad (10)$$

and

$$\begin{cases} V_{ds} = 0 \\ V_{qs} = V_s = \omega_s \Phi_{ds} \end{cases} \quad (11)$$

The statoric power is controlled by the rotor voltages V_{rd} and V_{rq}, It is an independent control of active and reactive powers. In the d-q reference frame, the power can be written as:

$$\begin{cases} P_s = V_{qs} I_{qs} + V_{ds} I_{ds} = -V_s \frac{L_m}{L_s} I_{qr} \\ Q_s = V_{qs} I_{ds} - V_{ds} I_{qs} = V_s\left(\frac{\Phi_s}{L_s}\right) - V_s\left(\frac{L_m}{L_s}\right) I_{dr} \end{cases} \quad (12)$$

$$\begin{cases} V_{dr} = R_r I_{dr} + \left(L_r - \frac{L_m^2}{L_s}\right)\frac{dI_{dr}}{dt} - g\omega_s\left(L_r - \frac{L_m^2}{L_s}\right) I_{qr} \\ V_{qr} = R_r I_{qr} + \left(L_r - \frac{L_m^2}{L_s}\right)\frac{dI_{qr}}{dt} - g\omega_s\left(L_r - \frac{L_m^2}{L_s}\right) I_{dr} + g\left(\frac{L_m V_s}{L_s}\right) \end{cases} \quad (13)$$

V. Sliding Mode Controller

In recent years the sliding mode controller has been very successful, it has three main features:

- Simplicity of implementation
- Robustness against system uncertainties
- External disturbances affecting the process.

The basic idea of sliding mode control is first to draw the states of the system in an area properly selected, then design a law command that will always keep the system in this region [14]. The sliding mode control goes through three stages:

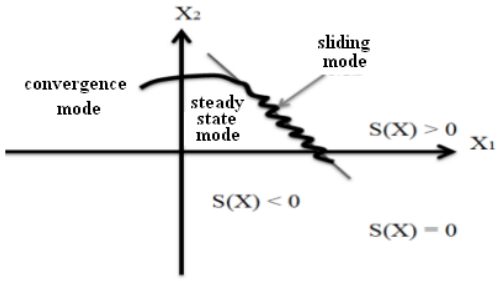

Fig. 3 Mode trajectory in phase plan

The sliding mode control consists to return the state trajectory towards the sliding surface and to develop it above, with a certain dynamics up to the equilibrium [10], [11]. Its design consists mainly to determine three stages [7]-[15].

A. The Switching Surface Choice

For a non-linear system represented by:

$$\begin{cases} \dot{X} = f(X,t) + g(X,t)u(X,t) \\ X \in \mathbb{R}^n, u \in \mathbb{R} \end{cases} \tag{14}$$

where f(X,t), g(X,t), are two continuous and uncertain non-linear functions, supposed limited. The general equation to determine the sliding surface given by [15], [16]:

$$\begin{cases} S(X) = (\frac{d}{dt} + \lambda)^{n-1} e \\ e = X^d - X \\ X^d = [x^d, \dot{x}^d, \ddot{x}^d, ...]^T \\ X = [x, \dot{x}, ..., , x^{n-1}]^T \end{cases} \tag{15}$$

where e is the size to resolve error, λ is positive coefficient, n is order of the system, X^d desire greatness.

B. Convergence Condition

The convergence condition is defined by the Lyapunov equation [7], [8], [15]; it makes the surface attractive and invariant.

$$S(X)\dot{S}(X) \le 0 \tag{16}$$

C. Control Calculation

The control algorithm is defined by the relation:

$$u = u^{eq} + u^n \tag{17}$$

where u is control signal, u^{eq} is equivalent control signal, u^n is switching control, sat (S(X)/φ) is Saturation function, u^{eq} can be obtained by considering the condition for the sliding regime:

$$S(X,t)=0. \tag{18}$$

The equivalent control keeps the state variable on sliding surface, once they reach it. u^n is needed to assure the convergence of the system states to sliding surfaces in finite time.

In order to alleviate the undesirable chattering phenomenon, J. J. Slotine proposed an approach to reduce it, by introducing a boundary layer of width φ on either side of the switching surface [17].

Then, u^n is defined by:

$$u^n = u^{\max} sat(S(X)/\varphi), \tag{19}$$

where sat(S(X)) is the proposed saturation function and defined by:

$$sat(S(X)/\varphi) = \begin{cases} sign(S) i |S| > \varphi \\ S/\varphi if\ |S| < \varphi \end{cases} \tag{20}$$

φ is the boundary layer width, u^{max} is the controller gain designed from the Lyapunov stability. Commonly, in DFIG control using sliding mode theory, the surfaces are chosen according of the error between the reference input signal and the measured signals [17].

D. Power Control

To control the power we set n=1, the expression of the active and reactive power control surface becomes:

$$\begin{cases} S(P) = (P_{sref} - P_s) \\ S(Q) = (Q_{sref} - Q_s) \end{cases} \tag{21}$$

The derivative of the surface is:

$$\begin{cases} \dot{S}(P) = (\dot{P}_{sref} - P_s) \\ \dot{S}(Q) = (\dot{Q}_{sref} - Q_s) \end{cases} \tag{22}$$

Replacing it in the power expression:

$$\begin{cases} \dot{S}(P) = (\dot{P}_{sref} + V_s \frac{L_m}{L_s} \dot{I}_{qr}) \\ \dot{S}(Q) = (\dot{Q}_{sref} - (-V_s \frac{L_m}{L_s} \dot{I}_{dr}) \end{cases} \tag{23}$$

Taking the current expression from the voltage equation:

$$\begin{cases} \dot{S}(P) = (\dot{P}_{sref} + V_s \frac{L_m}{L_r L_s \sigma} (V_{qr} - R_r \dot{I}_{qr})) \\ \dot{S}(Q) = (\dot{Q}_{sref} + V_s \frac{L_m}{L_r L_s \sigma} (V_{dr} - R_r \dot{I}_{dr})) \end{cases} \tag{24}$$

where

$$\sigma = (1 - \frac{L_m^2}{L_s L_r}) \tag{25}$$

We take

$$\begin{cases} V_{qr} = V_{qr}^{eq} + V_{qr}^{n} \\ V_{dr} = V_{dr}^{eq} + V_{dr}^{n} \end{cases} \quad (26)$$

$$\begin{cases} \dot{S}(P) = (\dot{P}_{sref} + V_s \dfrac{L_m}{L_r L_s \sigma}((V_{qr}^{eq} + \dot{V}_{qr}^{n}) - R_r I_{qr})) \\ \dot{S}(Q) = (\dot{Q}_{sref} + V_s \dfrac{L_m}{L_r L_s \sigma}((V_{dr}^{eq} + \dot{V}_{dr}^{n}) - R_r I_{dr})) \end{cases} \quad (27)$$

During the sliding mode and in permanent regime, we have:

$$\begin{cases} S(P)\dot{S}(P) \le 0 \\ S(Q)\dot{S}(Q) \le 0 \end{cases} \quad (28)$$

The equivalent control amount is found from the previous equations and written as:

$$\begin{cases} V_{qr}^{eq} = -\dot{P}_{sref} \dfrac{L_r L_s \sigma}{V_s L_m} + R_r I_{qr} \\ V_{dr}^{eq} = -\dot{Q}_{s}^{ref} \dfrac{L_r L_s \sigma}{V_s L_m} + R_r I_{dr} \end{cases} \quad (29)$$

During the convergence mode, so that the condition is:

$$\begin{cases} S(P) = 0, \dot{S}(P) = 0, V_{qr}^{n} = 0 \\ S(Q) = 0, \dot{S}(Q) = 0, V_{qr}^{n} = 0 \end{cases} \quad (30)$$

Verified, we set:

$$\begin{cases} S(P) = -V_s \dfrac{L_m}{L_r L_s \sigma} V_{qr}^{n} \\ S(Q) = -V_s \dfrac{L_m}{L_r L_s \sigma} V_{dr}^{n} \end{cases} \quad (31)$$

Therefore, the switching term is given by:

$$\begin{cases} V_{qr}^{n} = KV_{qr} \, \mathrm{sign} S(P) \\ V_{dr}^{n} = KV_{qr} \, \mathrm{sign} S(Q) \end{cases} \quad (32)$$

K_{Vqr} and K_{Vdr} are positive constant given in Table III.

VI. Backstepping Controller

A. Principe Technique Backstepping

The basic idea of the Backstepping design is the use of the so-called virtual control to systematically decompose a complex nonlinear control design problem into simpler smaller ones [18]. Roughly speaking, Backstepping design is divided into various design steps [19], [20]. In each step we essentially deal with an easier, single-input-single-output design problem, and each step provides a reference for the next design step. The overall stability and performance are achieved by a Lyapunov function for the whole system [18].

B. Application of Backstepping for Machine Control

Research on the development of the DFIG control technology has multiplied in recent decades. We currently find several techniques present in the literature, such as vector control, DTC, nonlinear controls such as Backstepping and control sliding mode [21].

C. Power Control

We define the errors e_1 and e_2 representing the error between the actual power P_s and the reference power P_{ref} and the error between reactive power Q_s and its reference Q_{ref}

$$\begin{cases} e_1 = P_{ref} - P_s \\ e_2 = Q_{ref} - Q_s \end{cases} \quad (33)$$

The derivative of this equation gives:

$$\begin{cases} \dot{e}_1 = \dot{P}_{ref} - \dot{P}_s \\ \dot{e}_2 = \dot{Q}_{ref} - \dot{Q}_s \end{cases} \quad (34)$$

$$\begin{cases} \dot{e}_1 = \dot{P}_{ref} + V_s \dfrac{M}{L_s} \dot{I}_{qr} \\ \dot{e}_2 = \dot{Q}_{ref} + V_s \dfrac{M}{L_s} \dot{I}_{dr} \end{cases} \quad (35)$$

The first Lyapunov function is chosen so such that:

$$V_1 = \frac{1}{2}(e_1^2 + e_2^2) \quad (36)$$

Its derivative is:

$$\dot{V}_1 = e_1 \dot{e}_1 + e_2 \dot{e}_2 \quad (37)$$

$$\dot{V}_1 = e_1(\dot{P}_{ref} - \dot{P}_s) + e_2(\dot{Q}_{ref} - \dot{Q}_s) \quad (38)$$

$$\dot{V}_1 = e_1 \left[\dot{P}_{ref} + \frac{L_m V_s}{L_s} \left(V_{qr} - R_r I_{qr} - g\omega_s \beta I_{dr} - g \frac{L_m V_s}{L_s} \right) \frac{1}{\alpha} \right] + e_2 \left[\dot{Q}_{ref} + \frac{L_m V_s}{L_s} \left(V_{dr} - R_r I_{dr} - g\omega_s \beta I_{qr} \right) \frac{1}{\alpha} \right] \quad (39)$$

The pursuits of goals are achieved by choosing the references of the current components representing the stabilizing functions as:

$$\begin{cases} I_{qrref} = X \left[k_1 e_1 + \dot{P}_{ref} + \dfrac{L_m V_s}{L_s \alpha} \left(V_{qr} - g\omega_s \beta I_{dr} - g \dfrac{L_m V_s}{L_s} \right) \right] \\ I_{drref} = X \left[k_2 e_2 + \dot{Q}_{ref} + \dfrac{L_m V_s}{L_s \alpha} \left(V_{dr} + g\omega_s \beta I_{qr} \right) \right] \end{cases} \quad (40)$$

with:

$$X = \frac{L_s \alpha}{V_s L_m R_r}, \beta = L_s - \frac{L_m^2}{L_s}, \alpha = L_r - \frac{L_m^2}{L_s}$$

where k_1 and k_2 are positive constants given in Table IV (Appendix). The derivative of the Lyapunov function becomes:

$$\dot{V}_1 = -k_1 e_1^2 - k_2 e_2^2 \quad (41)$$

So, I_{qrref} and I_{drref} in (40) are asymptotically stable. We define the errors e_3 and e_4 respectively representing the error between I_{qr} and his reference I_{qrref}, I_{dr} and his reference I_{drref}

$$\begin{cases} e_3 = I_{qrref} - I_{qr} \\ e_4 = I_{drref} - I_{dr} \end{cases} \tag{42}$$

The derivative of this equation gives:

$$\begin{cases} \dot{e}_3 = \dot{I}_{qrref} - \dot{I}_{qr} \\ \dot{e}_4 = \dot{I}_{drref} - \dot{I}_{dr} \end{cases} \tag{43}$$

$$\begin{cases} \dot{e}_3 = \dot{I}_{qrref} - \frac{1}{\alpha} V_{qr} - S_1 \\ \dot{e}_4 = \dot{I}_{drref} - \frac{1}{\alpha} V_{dr} - S_2 \end{cases} \tag{44}$$

with

$$S_1 = \frac{1}{\alpha}\left(R_r I_{qr} - g\omega_s \beta I_{dr} - g\frac{L_m V_s}{L_s} \right) \tag{45}$$

$$S_2 = \frac{1}{\alpha}\left(- R_r I_{dr} + g\omega_s \beta I_{qr} \right) \tag{46}$$

Actual control laws of the machine V_{dr} and V_{qr} shown in (44), then we can go to the final step.

The final Lyapunov function is given by:

$$V_2 = \frac{1}{2}(e_1^2 + e_2^2 + e_3^2 + e_4^2) \tag{47}$$

The derivative of equation is given by:

$$\dot{V}_2 = e_1\dot{e}_1 + e_2\dot{e}_2 + e_3\dot{e}_3 + e_4\dot{e}_4 \tag{48}$$

This can be rewritten as:

$$\begin{aligned} \dot{V}_2 &= -k_1 e_1^2 - k_2 e_2^2 - k_3 e_3^2 - k_4 e_4^2 \\ &+ e_3\left(k_3 e_3 + \dot{I}_{qrref} - \frac{1}{\alpha} V_{qr} - S_1 \right) + e_4\left(k_3 e_3 + \dot{I}_{drref} - \frac{1}{\alpha} V_{dr} - S_2 \right) \end{aligned} \tag{49}$$

where k_3 and k_4 are positive constants given in the Appendix (Table IV). Control voltages V_{dr} and V_{qr} are selected as:

$$\begin{cases} V_{qr} = \alpha\left(k_3 e_3 + \dot{I}_{qrref} - S_1 \right) \\ V_{dr} = \alpha\left(k_4 e_4 + \dot{I}_{drref} - S_2 \right) \end{cases} \tag{50}$$

which ensures that $\dot{V}_2 < 0$. The stability control is obtained by a good choice of gains: k_1, k_2, k_3 and k_4.

VII. Simulations And Results

Simulations of SMC and BSC control strategy for a DFIG based wind power generation system were carried out, using MATLAB/Simulink, and Fig. 1 shows the scheme of the implemented system. The DFIG is rated at 1.5 MW with its parameters given in Table I. The nominal converter dc-link voltage was set at 1400 V.

A. Reference Tracking

The machine speed is attached to 1600 rpm in ideal conditions, the active power reference P_{ref} is 0.75MW and 1.5MW (supply of power to the network). The reactive power reference Q_{ref} is -0.5MVAR (inductive), 0.25MVAR (capacitive) and 0MVAR (cosφ=1). Figs. 4 and 5 show the response of active and reactive power for DFIG by the SMC and BSC controller, Fig. 6 shows the rotoric and statoric currents.

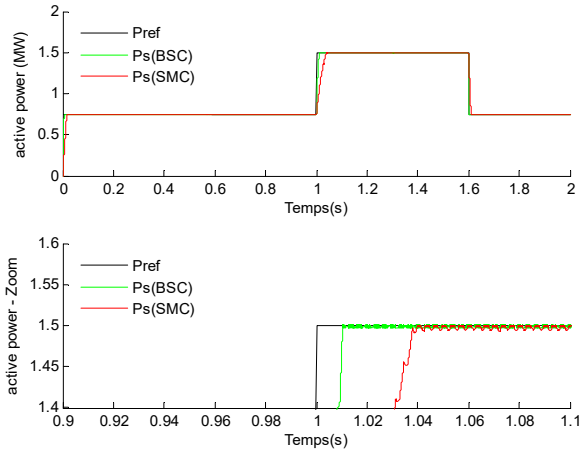

Fig. 4 Response to the active and reactive power with SMC and BSC

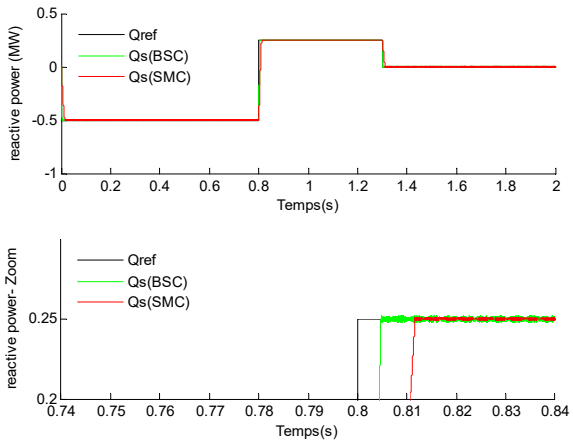

Fig. 5 Response to the reactive and reactive power with SMC and BSC

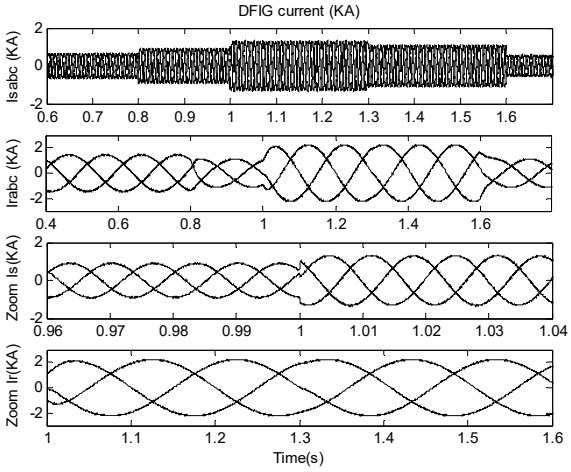

Fig. 6 Statoric and rotoric current for DFIG

From the figure, we can conclude a quicker response for BSC, and the answers are without overshoots, no effect coupling between two axes. The negative sign of the reactive power shows that the generator functions in capacitive mode, for inductive mode the power becomes automatically positive. In the end, the decoupling between the two axis is perfectly respected.

To reduce any possible overshoot of the reference voltage V_{qr}, it is often useful to add a voltage limiter.

B. Robustness Test

The parameters of the system are subject to changes driven by different physical phenomen, so our controller should provide good control whatever the variation of the generator parameters. In order to test the robustness of the controller we varied the rotor resistance R_r to $1.5R_r$, and the inductance value of the rotor and stator decreased by 10% from its nominal value. Fig. 7 shows the effect of varying the parameters of the generator R_r, L_s, L_r and L_m on the response of the active and reactive power.

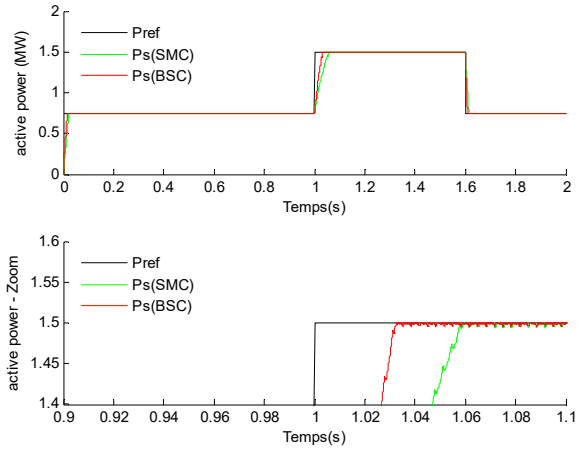

Fig. 7 Active power with parametres variations (Rr to 1.5Rr, Lr and Ls decreased by 10%, Lm decreased by 10%)

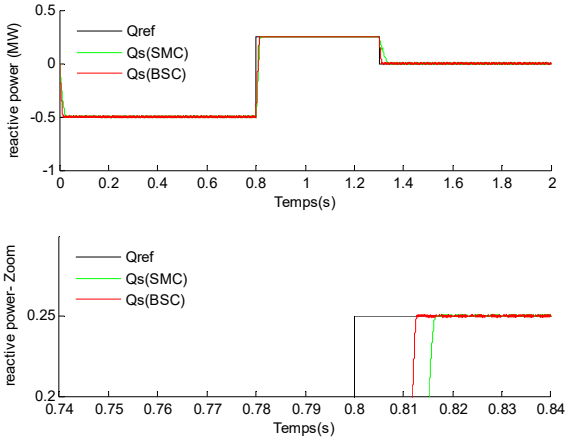

Fig. 8 Reactive power with parametres variations (Rr to 1.5Rr, Lr and Ls decreased by 10%, Lm decreased by 10%)

From simulation results, we found that the BSC is more robust, the response time is almost the same despite changes in the parameters of the DFIG.

VIII. Conclusion

The work presented in this paper devoted to power control of DFIG used in wind turbine by the sliding mode controller, after modeling the DFIG in the d and q axis, we have established a vector control of DFIG based in stator flux oriented, then the SMC are synthesized and compared to a conventional PI controller.

We have presented the performance of the BSC and SMC and compared between them, the robustness of the controllers is evaluated and allows us to have a decoupling between active and reactive power thus independent control.

The simulation results show that the BSC is much more efficient compared to SMC, it also improves the performance of the DFIG, and ensure some important strength despite the variation of the parameters of the DFIG.

Appendix

TABLE I
DFIG Parameters

Symbol	Quantity	Value
P	Rated power	1.5MW
Vs	Statoric voltage	690V – 50Hz
Vs	Rotoric voltage	389V-14Hz
Rs	Statoric resistance	0.012Ω
Rs	Rotoric resistance	0.021 Ω
Ls	Statoric inductance	0.0137 H
Lr	Rotoric inductance	0.0136H
L_m	mutual inductance	0.0135H
P	Pole pairs	2
F	The friction Coefficient	0.024N.m.s^{-1}
J	The moment of inertia	1000 kg.m^2

TABLE II
Turbine Parameters

Symbol	Quantity	Value
R	Radius of the wind	35.25 m
G	Gain multiplier	0.48
ρ	Air density	1.225kg/m^3

TABLE III
SMC PARAMETERS

Symbol	Value	Unit
K_{Vqr}	5000	Without
K_{Vqr}	1800	Without

TABLE IV
BSC PARAMETERS

Symbol	Value	Unit
k_1	8060	Without
k_2	5000	Without
k_3	3590	Without
k_4	6000	Without

REFERENCES

[1] Beltran, B., Ahmed-Ali, T., Benbouzid, M., "Sliding mode power control of variable speed wind energy conversion systems". IEEE Trans. Energy Conversion, vol. 23, n°2, pp. 551-558, June 2008.
[2] Beltran, B. "Maximisation de la Puissance Produite par une Génératrice Asynchrone Double Alimentation d'une Eolienne par Mode Glissant d'Ordre Supérieur". JCGE'08 LYON, 16 et 17 décembre 2008
[3] Abad, G., Rodriguez, M. A., Poza, J., "Predictive Direct Power Control of the Doubly Fed Induction Machine with Reduced Power Ripple at Low Constant Switching Frequency". IEEE International Symposium on Industrial Electronics, ISIE, June 2007, pp. 1119-1124.
[4] Boulahia, A., Nabti, K., Benalla, H., "Direct power control for AC/DC/AC converters in Doubly Fed Induction Machine based wind turbine". Journal of Theoretical and Applied Information Technology (JATIT), 15th May 2012. Vol. 39 No.1.
[5] Berra, A., Ouadi, H., "Sensorless speed and reactive power control of a DFIG-wind turbine". Journal of Theoretical and Applied Information Technology (JATIT), 20th April 2014. Vol. 62 No.2.
[6] J.J.Slotine, "Adaptive Sliding controller synthesis fornonlinear systems », IJC, Vol 43 .N°6 1986, pp 1631-1638
[7] A. Belabbes, B. Hamane, M. Bouhamida, and A. Draou, "Power Control of a Wind Energy Conversion System based on a Doubly Fed Induction Generator using RST and Sliding Mode Controllers", International Conference on Renewable Energies and Power Quality, Santiago de Compostela-Spain, March, 2012
[8] Sid Ahmed El Mahdi Ardjoun, Mohamed Abid, Abdel Ghani AISSAOUI, Abedelatif Naceri, " A robust fuzzy sliding mode control applied to the double fed induction machine", international journal of circuits, systems and signal processing, Issue 4, Volume 5, 2011, pp 315-321.
[9] L. Xu, W. Cheng, "Torque and reactive power control of a doubly-fed induction machine by position sensorless scheme.", IEEE Transactions on Industry Applications, Vol. 31, N°3, pp 636-642, May/June 1995.
[10] Abdellah Boualouch, Abdellatif Frigui, Tamou Nasser, Ahmed Essadki, Ali Boukhriss, "Control of a Doubly-Fed Induction Generator for Wind Energy Conversion Systems by RST Controller." , International Journal of Emerging Technology and Advanced Engineering IJETAE, Volume 4, Issue 8, August 2014 pp 93-99.
[11] Fatma Hachicha, Lotfi Richen," Performance Analysis of a Wind Energy Conversion System based on a Doubly-Fed Induction Generator", IEEE Trans, 8th International Multi-Conference on Systems, Signals & Devices, 2011, pp 978-984.
[12] Pea, R, Cerdenas, R, Proboste, J, Asher, G., Clare, J ''Sensorless "Control of Doubly-Fed Induction Generators Using a Rotor-Current-Based MRAS Observer '' IEEE Transactions on Industrial Electronics, Vol. 55, no. 1, pp. 330 - 339, January 2008.
[13] M. Machmoum, F. Poitiers, C. Darengosse and A. Queric, "Dynamic Performances of a Doubly-fed Induction Machine for a Variable-speed Wind Energy Generation," IEEE Trans. Power System Technology, vol. 4, Dec. 2002, pp. 2431-2436.
[14] L. Zhang, C. Watthansarn and W. Shehered: "A matrix converter excited doubly-fed induction machine as a wind power generator, ", IEEE Trans. Power Electronics and Variable Speed Drives, vol. 2, 06august 2002,pp 532–537.
[15] J.J.Slotine, "Adaptive Sliding controller synthesis fornonlinear systems », IJC, Vol 43 .N°6, 1986, pp 1631-1651.
[16] Slotine, J.J.E. Li, Applied nonlinear control, Prence Hall, USA, 1998.
[17] V. I. Utkin, "Sliding mode control design principles and applications to electric drives", IEEE Trans. Ind. electronic, vol. 40, pp.2336, Feb.1993.
[18] M.Loucif, A.Boumediene and A.Mechernene, "Backstepping Control of Double Fed Induction Generator Driven by Wind Turbine," International Conference on Systems and Control, Algiers, Algeria, October-29-31, 2013.
[19] A. Laoufi, A. Hazzab, I.K. Bousserhane and M. Rahli Direct Field-Oriented control using Backstepping technique for Induction Motor speed control, International Journal of Applied Engineering Research vol. 1,pp. 37-50, 2006.
[20] M.R Jovanovic, B. Bamieh, Architecture Induced by Distributed Backstepping Design, IEEE Transactions on Automatic Control, Vol. 52, Issue. 1, pp. 108-113, January 2007.
[21] A.Elmansouri, J.El mhamdi and A.Boualouch," Control by Backstepping of the DFIG used in the wind turbine." , International Journal of Emerging Technology and Advanced Engineering IJETAE, Volume 5, Issue 2, February 2015, pp 472-478.

A. Boualouch received a Licence degree in 2010 and a Master degree in 2012 From ENSET School, Mohamed V University, Rabat. He is currently working toward the Ph.D degree in electrical engineering research at ENSET, Mohamed V University Rabat.

A. Essadki is currently a Professor and university research professor at the electrical engineering department of ENSET, Mohamed V University, Morocco. In 2000, He received his PhD degree from Mohammadia Engineering School (EMI), (Morocco). From1990 to 1993, he pursued his Master program at UQTR University, Quebec Canada, respectively, all in electrical engineering. His current research interests include renewable energy, motor drives and power system. Doctor Ahmed Essadki is a member of RGE Lab in research group leader.

T. Nasser is currently an Associate Professor at the communication networks department of National High School for Computer Science and Systems (ENSIAS), Mohamed V University, Morocco, since 2009. She received her PhD degree in 2005 and her research MS degree, in 2000, respectively, all in electrical engineering from Mohammadia Engineering School (EMI), Morocco. Her research interests are renewable energy, motor drives, power system She is a member of Al Jazari research group.

A. Boukhriss received a License degree from Enset School, Mohamed V University Rabat, and a master degree from Ensa School, Ibn Zohr University Agadir in 2011. He is currently working toward the PhD degree in electrical engineering research at Enset, Mohamed V University Rabat, Morocco.

A. Frigui received a Licence degree From Ben M'sek university, Casablanca in 2010 and a Master degree in 2012 From Enset school, Mohamed V University, Rabat. He is currently working toward the Ph.D degree in electrical engineering research at Enset, Mohamed V University, Rabat.